J. Biochem. **127**, 383–391 (2000)

Crystal Structure of Alkalophilic Asparagine 233–Replaced Cyclodextrin Glucanotransferase Complexed with an Inhibitor, Acarbose, at 2.0 Å Resolution

Noriyuki Ishii,*[,1] Keiko Haga,[†] Kunio Yamane,[†] and Kazuaki Harata*

**Biophysical Chemistry Laboratory, National Institute of Bioscience and Human-Technology, Tsukuba, Ibaraki 305-8566; and [†]Institute of Biological Sciences, University of Tsukuba, Tsukuba, Ibaraki 305-8572*

Received October 15, 1999; accepted December 2, 1999

The product specificity of cyclodextrin glucanotransferase (CGTase) from alkalophilic *Bacillus* sp. #1011 is improved to near-uniformity by mutation of histidine-233 to asparagine. Asparagine 233–replaced CGTase (H233N-CGTase) no longer produces α-cyclodextrin, while the wild-type CGTase from the same bacterium produces a mixture of predominantly α-, β-, and γ-cyclodextrins, catalyzing the conversion of starch into cyclic or linear α-1,4–linked glucopyranosyl chains. In order to better understand the protein engineering of H233N-CGTase, the crystal structure of the mutant enzyme complexed with a maltotetraose analog, acarbose, was determined at 2.0 Å resolution with a final crystallographic *R* value of 0.163 for all data. Taking a close look at the active site cleft in which the acarbose molecule is bound, the most probable reason for the improved specificity of H233N-CGTase is the removal of interactions needed to form a compact ring like α-cyclodextrin.

Key words: acarbose, CGTase, crystal structure, cyclodextrin glucanotransferase, X-ray crystallography.

Cyclodextrin glucanotransferase (EC 2.4.1.19, CGTase) is a bacterial enzyme that catalyzes the conversion of starch into cyclic or linear α-1,4–linked glucopyranosyl chains. The cyclic compounds are called cyclodextrins (CD) and, in general, they consist of six, seven, or eight D-glucopyranose units, which are referred to as α-, β-, γ-cyclodextrins, respectively (*1*). One property of CDs is their ability to form inclusion complexes with a variety of guest molecules, capturing them within the axial cavity of the molecule (*2*, *3*). Due to this useful feature of CDs, they have been utilized industrially and have attracted keen interest from many researchers in the fields of pharmaceuticals, chemicals, food industries, and so on. The isolation and characterization of CGTases from several kinds of bacteria such as *Bacillus circulans* (*4–6*), *B. stearothermophilus* (*7*, *8*), *B. macerans* (*9*), *B. autolyticus* (*10*), *Bacillus* sp. #1011 (*11–13*), and *Thermoanaerobacterium thermosulfurigenes* EM1 (*14*, *15*) have been reported. The CGTase from the alkalophilic bacterium (*Bacillus* sp. #1011) also possesses a common feature that is recognized in other CGTases from the different sources mentioned above. That is, CGTase produces a mixture consisting mainly of α-, β-, γ-CDs. Usually the products contain a mixture of several kinds of CDs and linear oligosaccharides. Since the complex-forming activity differs among CDs, further purification is required prior to use (*16*). However, a mutation at residue 233 changes the nature of the enzyme such that H233N-CGTase does not produce α-CD. This is a favorable step toward the design of a mutant that produces a single product. In order to better understand how the product specificity is improved in the H233N mutant, we examined previously determined X-ray crystal structures of CGTases from *Bacillus stearothermophilus* (*7*, *17*); *B. circulans* strain 8 (*18*, *19*), and strain 251 (*20*); alkalophilic *Bacillus* sp. #1011 (*21*, *22*); and *Thermoanaerobacterium thermosulfurigenes* EM1 (*14*). We also examined the structures of CGTases from *B. stearothermophilus* complexed with maltose (*7*); the enzyme from *B. circulans* strain 251 complexed with an analog like maltotetraose (*23*) as well as its mutant enzyme complexed with α-CD (*20*) and its inactive mutant from *B. circulans* strain 8 complexed with a derivative of β-CD (*24*). Although the 2.5 Å crystal structure of a CGTase with acarbose bound at the active site has been reported (*23*), as well as a structure of CGTase with a bound maltononaose inhibitor [apparently derived from condensation of maltononaose and acarbose (*25*)], a straightforward explanation for the increased product specificity of H233N-CGTase could not be found. Therefore, we determined the crystal structure of H233N-CGTase at 1.9 Å resolution (to be published elsewhere), and its complex formed with an inhibitor, acarbose (maltotetraose analog), at 2.0 Å. The most probable answer to the question appears to lie in the altered association between the substrate molecule and residue 233, and on the difference in conformation of the bound acarbose molecules seen at the active site clefts of the two independent H233N-CGTase molecules in an asymmetric unit.

[1]To whom correspondence should be addressed. Fax: +81-298-61-6194, E-mail: ishii@nibh.go.jp

Abbreviations: CD, cyclodextrin; CGTase, cyclodextrin glucanotransferase; H233N-CGTase, mutant CGTase of His233 to Asn; PEG, polyethylene glycol; F_o, observed structure factor amplitude; F_c, calculated structure factor amplitude; V_m, crystal volume per unit of protein molecular weight.

MATERIALS AND METHODS

Preparation and Crystallization—The alkalophilic H233N-CGTase was expressed in *Escherichia coli* cells and purified by the same procedure employed for the wild-type CGTase (*11*). In order to obtain the crystals of interest (the complex of alkalophilic H233N-CGTase with acarbose), H233N-CGTase (10 mg/ml) was co-crystallized in the presence of 0.4 mM acarbose. The crystals of the complex were grown over 1–2 weeks by the hanging drop vapor diffusion method at room temperature against a reservoir solution of 100 mM sodium citrate buffer (pH 5.6) containing 20% (w/v) PEG3000 and 20% (v/v) isopropanol.

Data Collection—Crystals of the complex of H233N-CGTase with bound acarbose molecules diffracted X-rays beyond 2.0 Å. The diffraction data were collected up to 1.86 Å in resolution with an Enraf-Nonius FAST diffractometer equipped with a DEP image intensifier and a FR571 generator, which was operated at 40 kV, 50 mA, and with a focal spot size of 0.2 mm. Seven sets of independent reflections were obtained from two crystals, and the data were merged into a set of 95,583 unique reflections with an R_{merge} (I) value of 0.088. Data completeness was 92.7% in the resolution range up to 2.0 Å.

Structure Determination and Refinement—The electron density map of acarbose-bound H233N-CGTase was calculated using the coordinates of H233N-CGTase previously built from the coordinates of the wild-type CGTase from the same bacterium. The positions and configurations of the acarbose molecules were assigned using both $2F_o$–F_c and F_o–F_c maps. The structure was refined using the program *X-PLOR* (*26*). During refinement, a simulation with slow-cooling molecular dynamics was carried out at 1,000 K (50 cycles for each step, step size 0.0005) for the data from 2.2 to 5.0 Å resolution, followed by energy minimization (120 cycles for the coordinate) using the 2.0–10 Å resolution data with $|F_o| > 2\sigma(F)$. The orientation of the side chain groups was corrected on a $2F_o$–F_c map. Positions of water molecules were determined from F_o–F_c and $2F_o$–F_c maps by their intensities in electron density (larger than 3σ in F_o–F_c map) and by intermolecular contacts (2.5–3.3 Å) with appropriate amino acids. Densities with B values higher than 60 Å^2 were discarded during refinement. The calculation of map and cycles of energy minimization, followed by the examination of F_o–F_c and $3F_o$–$2F_c$ maps, was continued until the refinement converged to an R value of 0.163 for 58,118 reflections with $|F_o| > 2\sigma(F)$ (R_{free} = 0.222).

RESULTS AND DISCUSSION

Determination and Refinement of the Structure—The crystals belonged to the triclinic space group $P1$ with cell dimensions of a = 64.93 Å, b = 73.83 Å, c = 79.05 Å, α = 85.1°, β = 105.4°, and γ = 100.5°. The V_m value was 2.39 Å^3/Da and the solvent content was about 48.6%. Two independent molecules were assigned in an asymmetric unit. The coordinate error estimated from the Luzzati plot (*27*) was smaller than 0.2 Å (data not shown). On the Ramachandran plot (data not shown), the (φ, ψ) angles settled in the normal area, except those of Ala-152 and Tyr-195 (φ ≈ 50°, ψ ≈ –130°) (*28*). These structural features were the same as recognized for the wild-type CGTase (*22*). Two independent H233N-CGTase molecules were found in an asymmetric unit, each of which contained two calcium ions and an acarbose molecule at the active site cleft. Figure 1 shows the stereoview of the pseudo-dimeric molecules of H233N-CGTase complexed with acarboses. Calcium ions are shown

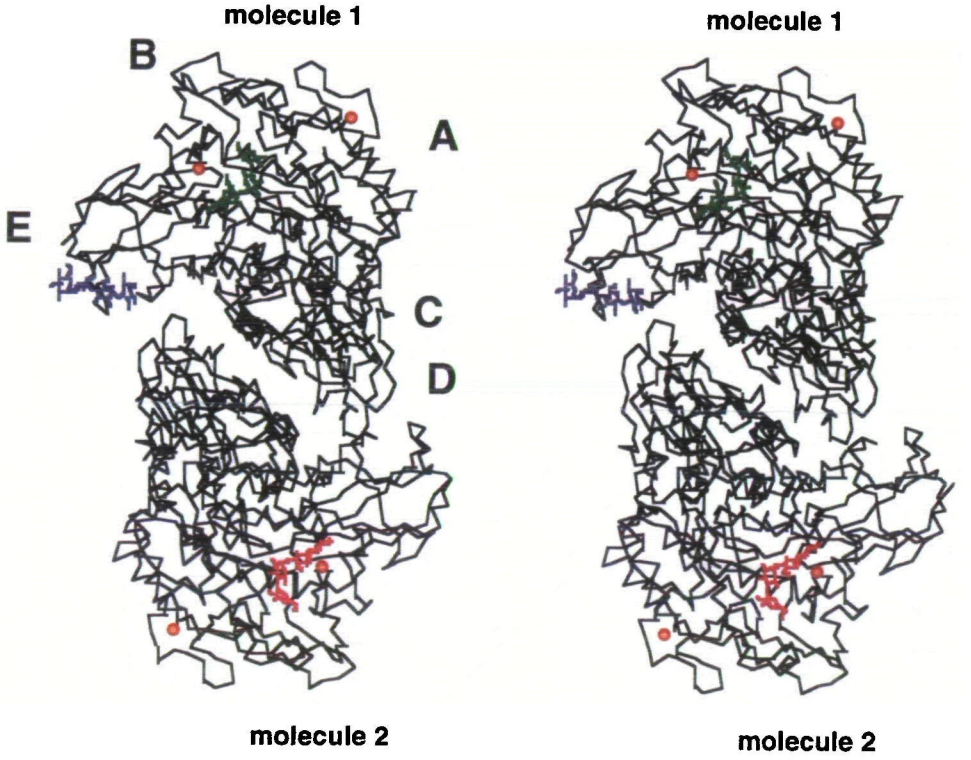

Fig. 1. **Stereoview of the backbone structure of H233N-CGTase complexed with acarbose molecules.** The two H233N-CGTase molecules are related by pseudo-twofold symmetry. The sub-domains in the protein are labeled A through E. The acarbose molecules captured in the active site clefts are shown in green for molecule 1, and in magenta for molecule 2. Another acarbose molecule bound at the sugar binding site on domain E of molecule 1 is shown in blue. The small red circles represent calcium ions that stabilize the protein structure.

in red. The bound acarbose molecules are indicated with different colors. The green and magenta are acarbose molecules that are captured at the active site cleft in molecule 1 and molecule 2, respectively. The blue is a bound molecule at another sugar-binding site reported on the domain E in molecule 1 (*20*, *25*). Interestingly, no corresponding molecule was observed in molecule 2. There are 759 water molecules that were assigned with full occupancy. Coordinates of the protein have been deposited with Protein Data Bank (entry code 1DED).

Comparison of Two Independent Acarbose-Bound Mutant Molecules in an Asymmetric Unit—The H233N-CGTase molecule consists of five domains (A: residues 1–138, 204–406, B: 139–203, C: 407–496, D: 497–584, E: 585–686). Two molecules are related by pseudo twofold symmetry (Fig. 1). The root mean square (r.m.s.) difference of the superimposed equivalent Cα coordinates between the two acarbose-bound H233N-CGTase molecules is 0.34 Å, indicating that the conformational changes in the two molecules upon the binding of acarbose are slightly different. When the inhibitor, acarbose, is bound to the active site cleft of the mutant enzyme, the r.m.s. difference for the Cα coordinates between the apo-enzyme and the acarbose-bound form of mol-

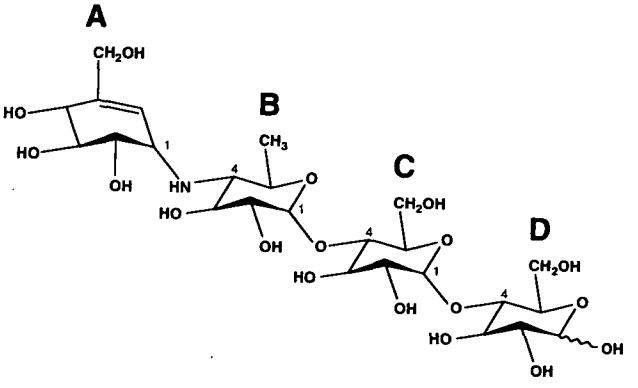

Fig. 3. **Structure of pseudo-tetrasaccharide acarbose.**

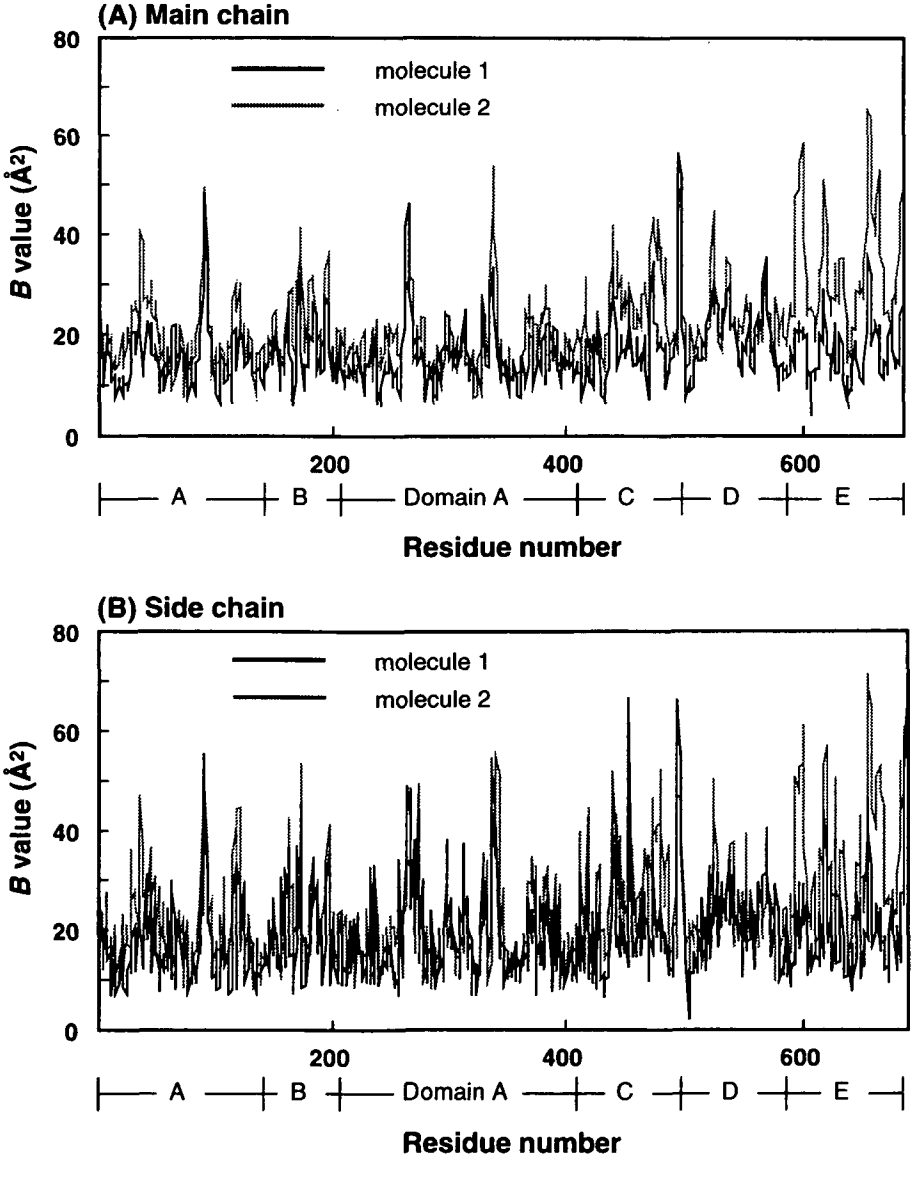

Fig. 2. **Plot of the average *B* value of the main-chain (A) and side-chain (B).**

ecule 1 and molecule 2 are both 0.23 Å.

The *B* values of the main chain and the side chain atoms of molecules 1 and 2 are shown in Fig. 2. The averaged *B* values in molecule 1 are 17.6 Å^2 for all atoms, 16.6 Å^2 for main chain atoms, and 18.6 Å^2 for side chain atoms. The corresponding values in molecule 2 are 23.3 Å^2 for all atoms, 22.7 Å^2 for main chain atoms, and 23.9 Å^2 for side chain atoms. The larger *B* values in molecule 2, especially

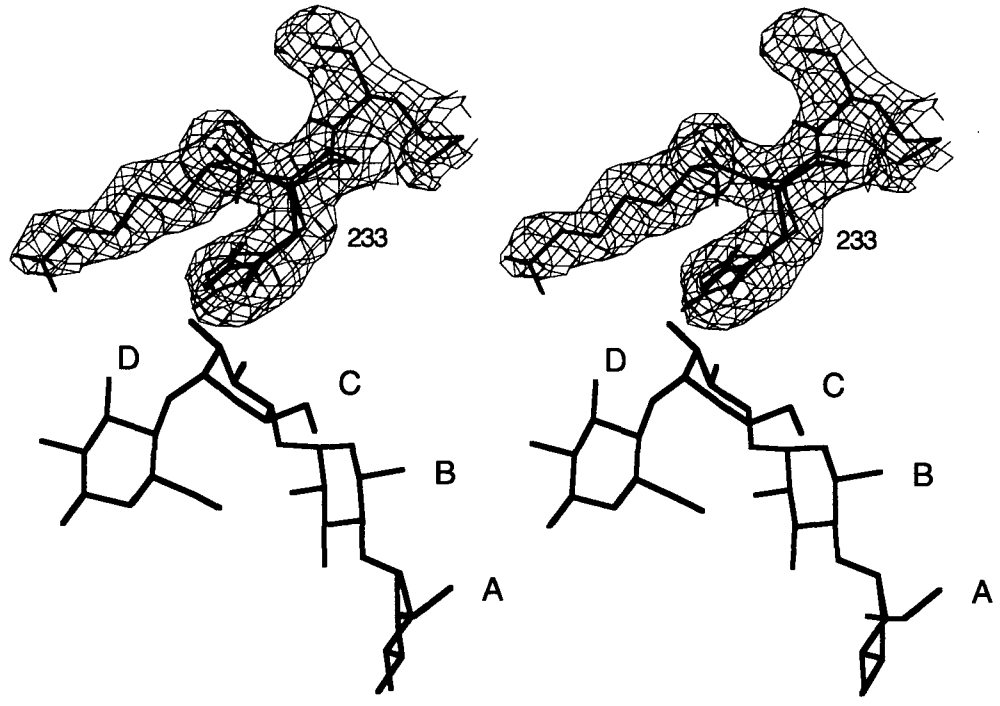

Fig. 4. **Stereopicture showing electron density for Asn-233 of H233N-CGTase molecule 1 in a 2.0 Å ($2F_o$–F_c) map contoured at 2.5σ.** His-233 for the wild-type is superimposed with thin solid lines. It can be seen that the side-chains of the residues are located close to residue C of an acarbose molecule bound at the active center.

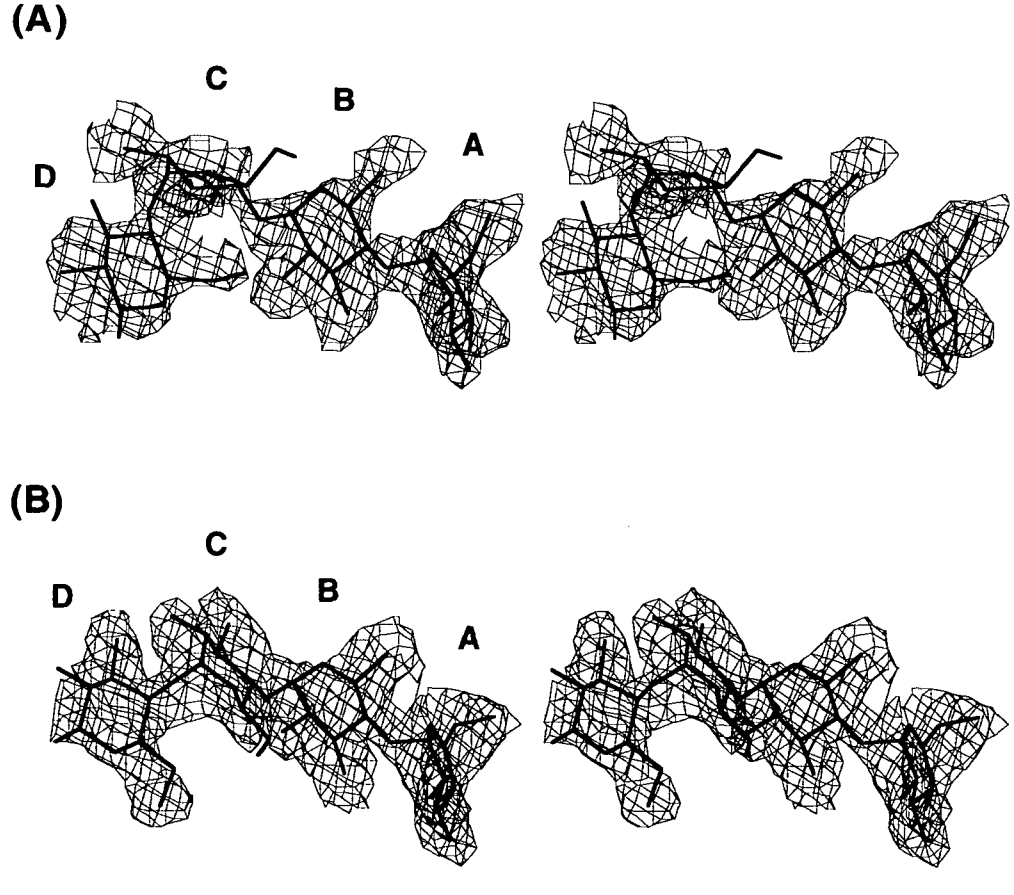

Fig. 5. **Stereoviews of electron density for acarbose molecules in the active center of H233N-CGTase molecule 1 (A) and molecule 2 (B) in a 2.0 Å ($2F_o$–F_c) omit map contoured at 2.5σ.** The residues in acarbose are labeled A through D.

in domain E, coincide with the fact that the domain contains another site for sugar binding (Fig. 2). Some external loop regions show slightly different conformations in the two molecules. Taking a close look at the secondary structure assigned by the program Procheck (*29*), it was found that molecule 1 consists of 21 α-helices and 37 β-strands, and that molecule 2 contains 21 α-helices and 35 β-strands. Differences were noticed in two regions; two β-strands are seen in the region from Asn-82 to Ala-102 of molecule 1, but there are no recognizable β-strands in the corresponding region of molecule 2. A short α-helix from Gly-36 to Ala-38 was seen in the acarbose-bound molecule 1, which was common to both molecules of the apo-H233N-CGTase, but it appeared shifted to the region from Pro-30 to Asn-32 in molecule 2. Fairly movable regions in the secondary structure are found near the bottom of the active site cleft. On examination of the two molecules in the context of neighboring molecules, it could be seen that one molecule of each pair lies fairly close to another molecule of a neighboring unit. Thus a part of the observed difference between the

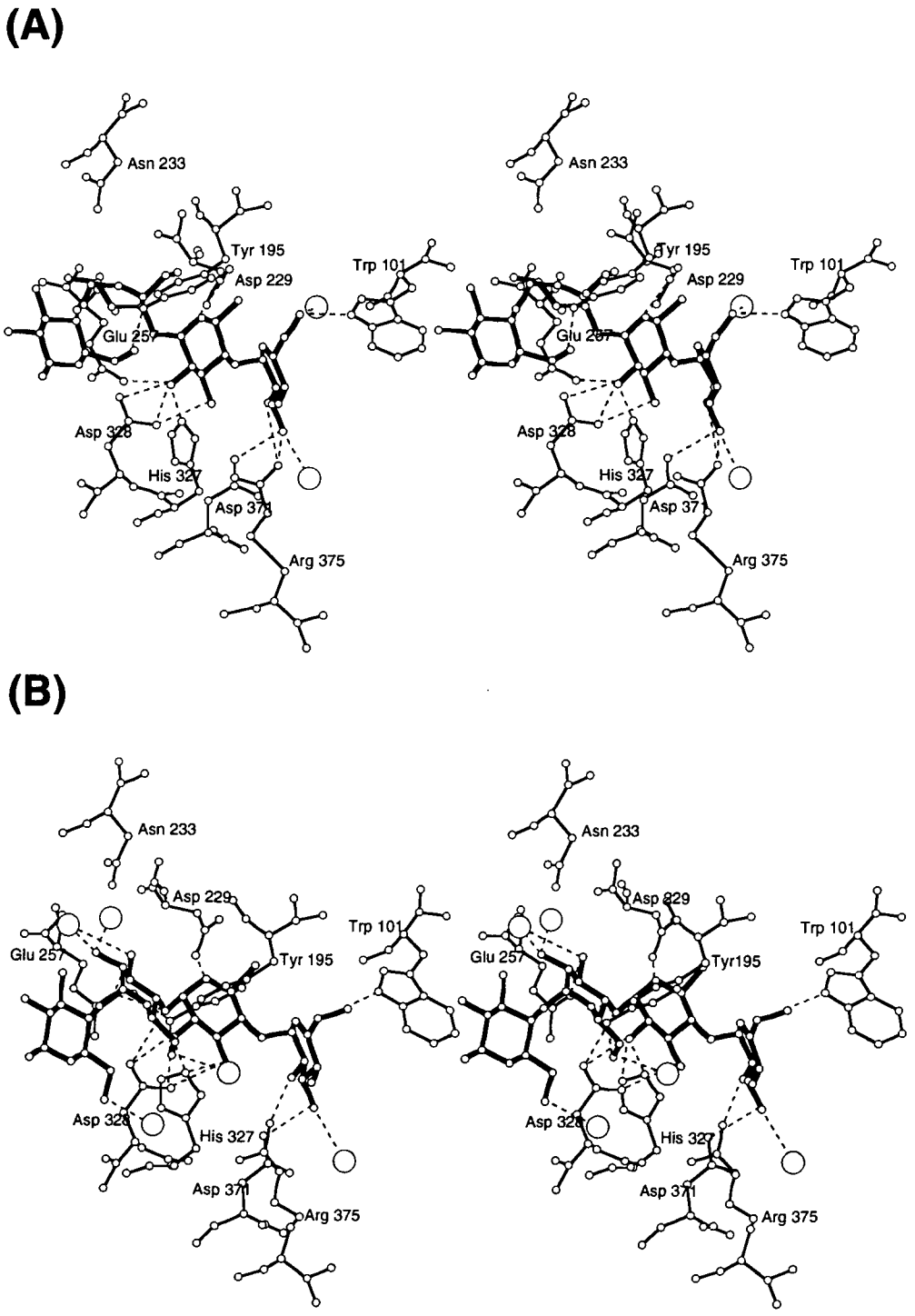

Fig. 6. **Stereoviews of the active site of molecule 1 (A) and molecule 2 (B) with bound acarbose molecules.** Water molecules are shown as large circles.

two molecules should be due to crystal packing.

Geometry around the Active Site Cleft and Role of Residue 233—The structure of the pseudo-tetrasaccharide acarbose molecule is shown in Fig. 3. Figure 4 shows a stereopicture of electron density for Asn-233 of H233N-CGTase molecule 1 in a 2.0 Å ($2F_o$–F_c) map. Residue 233 in the wild-type, His-233, is superimposed with thin solid lines. The orientation of the side-chain of residue 233 is important for interaction with the substrate. Asn-233 is located close to residue C of an acarbose molecule bound at the active center. The *B* value of Asn-233 is 10.6 Å^2 for molecule 1 and 19.6 Å^2 for molecule 2. The electron densities in the 2.0 Å ($2F_o$–F_c) map for acarbose molecules bound in the active center of H233N-CGTase molecule 1 and molecule 2 are shown in Fig. 5. The electron density of acarbose was calculated using both $2F_o$–F_c and F_o–F_c omit maps in H233N-CGTase. The electron density of the acarbose-bound H233N-CGTase was previously built using the Fourier components of the H233N-CGTase structure that contained no ligands. The fit of the acarbose residues to the electron density was reasonable in light of the weak affinity of acarbose for H233N-CGTase (K_i = 19 μM) (*12*). Recently a different binding mode for acarbose in the active center was reported by Mosi *et al.* (*31*). Though we tried to place the acarbose as they reported and then refine the structure, there was difficulty in fitting the conformation of the acarbose to our present electron density. To clarify this matter (*20*, *31*), it is necessary to collect diffraction data up to much higher resolution using cryogenic techniques. We are continuing to discuss using the currently prevailing model for acarbose binding. Figure 6, A and B, shows stereoviews of the geometry of the active site cleft with the bound acarbose. The structure found in molecule 1 is presented as Fig. 6A and that in molecule 2 is presented as Fig. 6B. Each acarbose molecule is seen to be significantly bent in the active site. As reported by Nakamura *et al.* (*11*) and Klein *et al.* (*19*), catalytically important residues such as Asp-229, Glu-257, and Asp-328 are recognized to interact through hydrogen bonds with the acarbose. Other residues such as Trp-101, Tyr-195, His-327, Asp-371, and Arg-375 also associate with the acarbose by hydrogen bonds. The manner of association of various residues with the acarbose are summarized schematically in Fig. 7. In Fig. 7, the acarbose molecules bound in molecule 1 and molecule 2 are superimposed so that the difference in conformation of the whole molecule, as well as a slight difference in the configuration

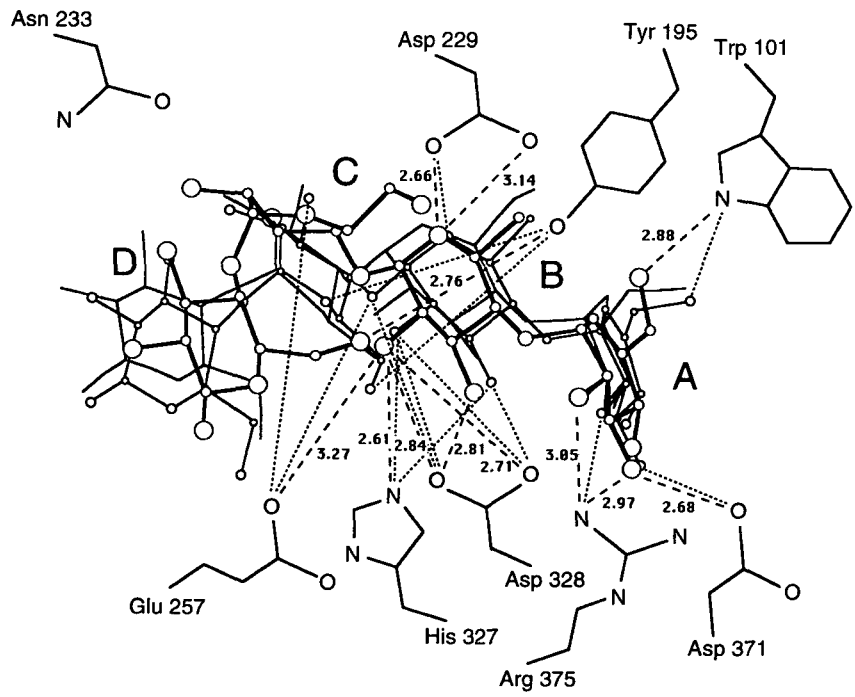

Fig. 7. **Schematic drawing of the geometry of the active site cleft with the acarbose molecules from molecule 1 and molecule 2 superimposed (green, molecule 1; magenta, molecule 2).** Hydrogen bonds are represented by dashed lines (thick line, molecule 1; thin line, molecule 2). Interatomic distances for acarbose in molecule 1 are given in Å. The other model for acarbose binding reported by Strokopytov *et al.* (*23*) is superposed in orange for reference.

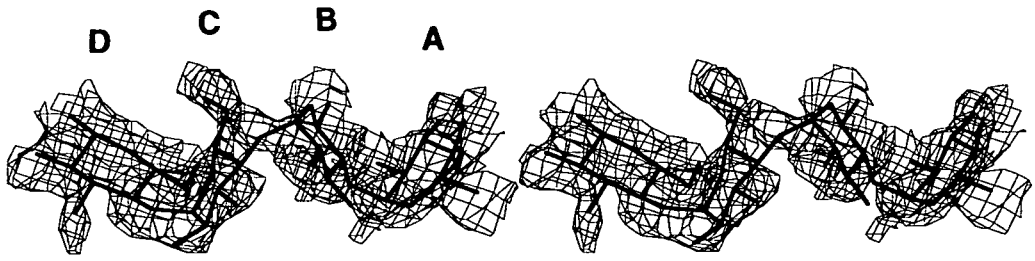

Fig. 8. **Stereodiagram showing electron density for an acarbose molecule on domain E of H233N-CGTase molecule 1 in a 2.0 Å ($2F_o$–F_c) omit map contoured at 1.4σ.** The residues in acarbose are labeled A through D.

of residue C between the two, can be easily recognized. As we hypothesized concerning the role of residue 233 in our previous report (*30*), our model can be proven to be correct by direct observation of the architecture of the active site cleft with the acarbose molecule. The Asn-233 residues are found to be about 3.6 Å away from the nearest glycopyranosyl ring of acarbose in molecule 1, and about 5.6 Å away in molecule 2, distances too large to allow association with the substrate by hydrogen bonds. The glycopyranosyl rings labeled A and B are overlap between the acarbose molecules of molecule 1 and molecule 2, but residues C and D are not located in the same orientation. This fact can be explained by our model which proposes that the absence of an interaction of residue 233 through hydrogen bonds to the substrate molecule allows the glycopyranosyl ring C to move freely. In particular, the mutation of His-233 to Asn shortens the side chain of residue 233 (Fig. 4) and reduces restraints on the substrate, thus changing the probable position of the glycopyranosyl ring C in the cleft. Since there is no interaction from Asn-233, residue C of the acarbose is no longer fixed in the active center. This is seen clearly in Fig. 7 as alternative positions for residues C and D of acarbose from molecule 1 and molecule 2. The weaker interaction with the enzyme at the positional sites around rings C and D, derived from the absence of restraint from Asn-233, appears to be the reason that H233N-CGTase no longer produces a compact ring like α-CD. A strong interaction between the protein and linear oligosaccharide substrates may be necessary to promote the cyclization reaction that produces further compact cyclic compounds.

Furthermore, another acarbose was found bound at another site in domain E of molecule 1. The electron density for this acarbose molecule in a 2.0 Å ($2F_o$–F_c) omit map is shown in Fig. 8. The fit of the residues of acarbose to the electron density seems to reflect the weak affinity of acarbose for the sugar binding site on domain E. The acarbose molecule is aligned with the two pyranose rings in parallel with Trp-616 and Trp-662, as is shown in Fig. 9. No corresponding molecule, however, was found in molecule 2. The difference can be understood to be due to slightly different molecular packing in the crystals. Figure 10 shows a schematic diagram of the H233N-CGTase residues in the domain that interacts by hydrogen bonds with the acarbose.

Possible polar contacts between the acarbose molecule and residues of the mutant enzyme at the active site clefts of both molecule 1 and molecule 2, and at the sugar binding site on domain E in molecule 1 are summarized (Table I). In clefts of both molecule 1 and molecule 2, the A and B residues of acarbose are tightly fixed by hydrogen bonds. The position of residue B is thought to be a cleavage site in hydrolysis, and the data show that the restraint on residue B seems very tight. In contrast to residue B, the positions of residues C and D are fairly loose. No hydrogen bonds are associated with residue C and just one hydrogen bond is

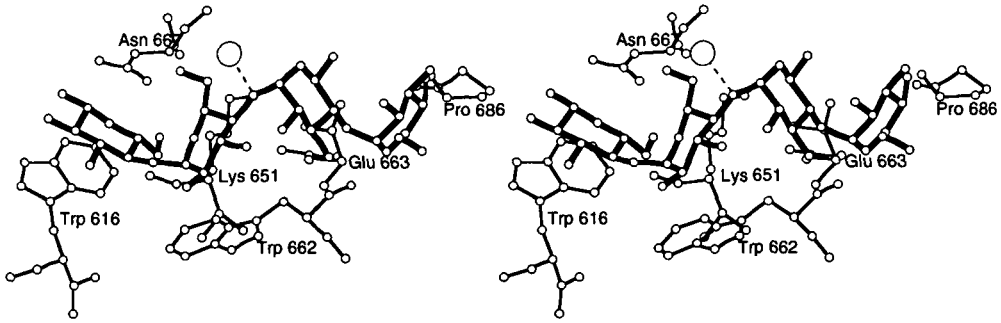

Fig. 9. **Stereoview of the sugar binding site on domain E of molecule 1 with acarbose.** Water molecules are shown as large circles.

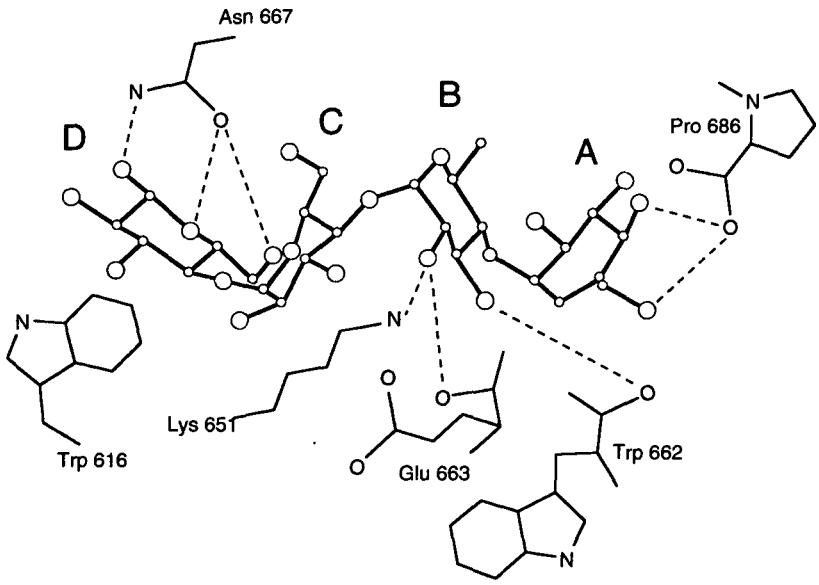

Fig. 10. **Schematic drawing of the geometry around the acarbose binding site on domain E in molecule 1.** Hydrogen bonds are represented by dashed lines.

TABLE I. **Possible polar contacts between acarbose and H233N-CGTase.**

Residue/atom	Protein atom	Distance (Å)	Residue/atom	Protein atom	Distance (Å)
At the active site cleft of H233N-CGTase molecule 1			At the active site cleft of H233N-CGTase molecule 2		
Residue A			Residue A		
O2	Arg375NH2	3.05	O2	Arg375NH2	2.83
O3	Asp371OD1	2.97	O3	Asp371OD1	2.87
O3	Arg375NH2	2.68	O6	Trp101NE1	3.01
O6	Trp101NE1	2.88	Residue B		
Residue B			O2	His327NE2	2.70
O2	His327NE2	2.61	O2	Asp328OD1	2.75
O2	Glu257OE2	3.27	O2	Asp328OD2	3.14
O2	Asp328OD1	2.84	O3	His327NE2	3.28
O2	Asp328OD2	2.71	O3	Asp328OD2	3.13
O3	Asp328OD1	2.81	O5	Asp229OD1	3.00
O5	Asp229OD1	2.66	Residue C		
O5	Asp229OD2	3.14	O3	Glu257OE2	2.79
Residue C			O4	Glu257OE2	3.04
None			O4	Asp328OD1	3.21
Residue D			O5	Tyr195OH	3.12
O6	Tyr195OH	2.76	O6	Tyr195OH	2.95
			Residue D		
			None		
At the sugar binding site on domain E of H233N-CGTase molecule 1					
Residue A					
O4	Pro686OT2	2.87			
O6	Pro686OT2	2.81			
Residue B					
O2	Lys651NZ	2.97			
O2	Glu663O	2.51			
O3	Trp662O	3.03			
Residue C					
None					
Residue D					
O1	Asn667ND2	3.25			
O5	Asn667OD1	3.25			
O6	Asn667OD1	2.54			

assigned to residue D in molecule 1. No interactions are seen for residue D in molecule 2, although residue C is held by five hydrogen bonds, including two interactions to O4 of residue C, in molecule 2 (Table I). It is interesting to see how residue 233, Asn-233, is located near the substrate. In molecule 1, the Asn-233 OD1 is located at a distance of 3.6 Å from O5 of the acarbose residue C, 4.2 Å from residue C O2, and 5.1 Å from residue C O6. In molecule 2, the Asn-233 OD1 lies 5.6 Å away from residue C O5. These distances are too large to form hydrogen bonds.

It is instructive to consider the role of residue 233 in enzymatic function. As reported previously (*12*), His-233 in the wild-type CGTase, which is one of the three histidines located near the active center, participates in the stabilization of the transition state rather than in substrate binding in the ground state. As reported by Mosi *et al.* (*31*), acarbose has the character of a transition state analog. In light of our results obtained by crystal structure analysis with bound acarbose, it may be that His-233 in the wild-type CGTase plays the role of a mediator to stabilize the substrate by forming hydrogen bonds. Replacement of His-233 by Asn has been reported to have a strong effect on the formation of β-CD as well as coupling and hydrolyzing activities (*12*). Although H233N-CGTase retains cyclization activities for cyclodextrins consisting of more than six glucopyranosides, such as β- and γ-CDs, no α-CD was detected even after long incubation. H233N-CGTase, however, retains α-CD hydrolyzing activity. This means that the mutation at residue 233 affects the formation of compact-cyclic products, but does not have a direct effect on the reverse hydrolysis. In other words, it can be said that the interaction between residue 233 and carbohydrates is critically important for CGTase to form compact CDs consisting of fewer than seven glucopyranose units, but that residue 233 is not directly concerned with the hydrolysis of CDs. The most likely role of the 233rd residue in the native enzyme, as deduced from the structural data, is that it associates with a substrate, oligosaccharide, so that the enzyme catalyzes the formation of a compact ring such as α-CD. In order to clarify the role of His-233 in the enzymatic function further, crystallographic analyses of the mutant CGTase complexed with a variety of different substrate molecule analogs are required. Structural information on mutations and modifications in the active site should be useful in designing CGTases with unique product specificities.

We gratefully thank Prof. Robert M. Glaeser, University of California, for helpful discussion and for critical reading of the manuscript.

REFERENCES

1. French, D. (1957) The schardinger dextrins. *Adv. Carbohydr. Chem.* **12**, 189–260
2. Schmid, G. (1989) Cyclodextrin glycosyltransferase production: yield enhancement by overexpression of cloned genes. *Trends Biotechnol.* **7**, 224–248
3. Szjitli, S. (1982) *Cyclodextrins and Their Inclusion Complexes*, Acadmiai Kiad, Budapest
4. Nitschke, L., Heeger, K., Bender, H., and Schulz, G.E. (1990) Molecular cloning, nucleotide sequence and expression in *Escherichia coli* of the β-cyclodextrin glycosyltransferase gene

from *Bacillus circulans* strain no. 8. *Appl. Microbiol. Biotechnol.* **33**, 542–546
5. Bovetto, L.J., Backer, D.P., Villette, J.R., Sicard, P.J., and Bouquelet, S.J.-L. (1992) Cyclomaltodextrin glucanotransferase from *Bacillus circulans* E 192, I. Purification and characterization of the enzyme. *Biotechnol. Appl. Biochem.* **15**, 48–58
6. Lawson, C.L., van Montfort, R., Strokopytov, B., Rozeboom, H.J., Kalk, K.H., deVries, G.E., Penninga, D., Dijkhuizen, L., and Dijkstra, B.W. (1994) Nucleotide sequence and X-ray structure of cyclodextrin glycosyltransferase from *Bacillus circulans* strain 251 in a maltose-dependent crystal form. *J. Mol. Biol.* **236**, 590–600
7. Kubota, M., Matsuura, Y., Sakai, S., and Katsube, Y. (1991) Molecular structure of *B. stearothermophilus* cyclodextrin glucanotransferase and analysis of substrate binding site. *Denpun Kagaku* **38**, 141–146
8. Tanaka, M., Muto, N., and Yamamoto, I. (1991) Characterization of *Bacillus stearothermophilus* cyclodextrin glucanotransferase in ascorbic acid 2-O-α-glucoside formation. *Biochim. Biophys. Acta* **1078**, 127–132
9. Abe, S., Nagamine, Y., Omichi, K., and Ikenaka, T. (1991) Investigation of the active site of *Bacillus macerans* cyclodextrin glucanotransferase by use of modified maltooligosaccharides. *J. Biochem.* **110**, 756–761
10. Tomita, K., Kaneda, M., Kawamura, K., and Nakanishi, K. (1993) Purification and properties of a cyclodextrin glucanotransferase from *Bacillus autolyticus* 11149 and selective formation of β-cyclodextrin. *J. Ferment. Bioeng.* **75**, 89–92
11. Nakamura, A., Haga, K., Ogawa, S., Kuwano, K., Kimura, K., and Yamane, K. (1992) Functional relationships between cyclodextrin glucanotransferase from an alkalophilic *Bacillus* and α-amylases. *FEBS Lett.* **296**, 37–40
12. Nakamura, A., Haga, K., and Yamane, K. (1993) Three histidine residues in the active center of cyclodextrin glucanotransferase from alkalophilic *Bacillus* sp. 1011: Effects of the replacement on pH dependence and transition-state stabilization. *Biochemistry* **32**, 6624–6631
13. Nakamura, A., Haga, K., and Yamane, K. (1994) The transglycosylation reaction of cyclodextrin glucanotransferase is operated by ping-pong mechanism. *FEBS Lett.* **337**, 66–70
14. Knegtel, R.M.A., Wind, R.D., Rozeboom, H.J., Kalk, K.H., Buitelaar, R.M., Dijkhuizen, L., and Dijkstra, B.W. (1996) Crystal structure at 2.3 Å resolution and revised nucleotide sequence of the thermostable cyclodextrin glycosyltransferase from *Thermoanaerobacterium thermosulfurigenes* EM1. *J. Mol. Biol.* **256**, 611–622
15. Wind, R.D., Uitdehaag, J.C.M., Buitelaar, R.M., Dijkstra, B.W., and Dijkhuizen, L. (1998) Engineering of cyclodextrin product specificity and pH optima of the thermostable cyclodextrin glycosyltransferase from *Thermoanaerobacterium thermosulfurigenes* EM1. *J. Biol. Chem.* **273**, 5771–5779
16. Szjitli, S. (1988) *Cyclodextrin Technology*, Kluwer Acad. Publ., Dordrecht
17. Kubota, M., Matsuura, Y., Sakai, S., and Katsube, Y. (1994) Three-dimensional structure of cyclodextrin glucanotransferase and its reaction mechanism. *Oyo Toshitsu Kagaku (J. Appl. Glycosci.)* **41**, 245–253
18. Klein, C. and Schulz, G.E. (1991) Structure of cyclodextrin glycosyltransferase refined at 2.0 Å resolution. *J. Mol. Biol.* **217**, 737–750
19. Klein, C., Hollender, J., Bender, H., and Schulz, E. (1992) Catalytic center of cyclodextrin glycosyltransferase derived from X-ray structure analysis combined with site-directed mutagenesis. *Biochemistry* **31**, 8740–8746
20. Knegtel, R.M.A., Strokopytov, B., Penninga, D., Faber, O.G., Rozeboom, H.J., Kalk, K.H., Dijkhuizen, L., and Dijkstra, B.W. (1995) Crystallographic studies of interaction of cyclodextrin glycosyltransferase from *Bacillus circulans* strain 251 with natural substrates and products. *J. Biol. Chem.* **270**, 29256–29264
21. Haga, K., Harata, K., Nakamura, A., and Yamane, K. (1994) Crystallization and preliminary X-ray studies of cyclodextrin glucanotransferase from alkalophilic *Bacillus* sp. 1011. *J. Mol. Biol.* **237**, 163–164
22. Harata, K., Haga, K., Nakamura, M., Aoyagi, M., and Yamane, K. (1996) X-ray structure of cyclodextrin glucanotransferase from alkalophilic *Bacillus* sp. 1011. Comparison of two independent molecules at 1.8 Å resolution. *Acta Cryst.* **D52**, 1136–1145
23. Strokopytov, B., Penninga, D., Rozeboom, H.J., Kalk, K.H., Dijkhuizen, L., and Dijkstra, B.W. (1995) X-ray structure of cyclodextrin glycosyltransferase complexed with acarbose. Implications for the catalytic mechanism of glycosidases. *Biochemistry* **34**, 2234–2240
24. Schmidt, A.K., Cottaz, S., Driguez, H., and Schulz, G.E. (1998) Structure of cyclodextrin glucanotransferase complexed with a derivative of its main product β-CD. *Biochemistry* **37**, 5909–5915
25. Strokopytov, B., Knegtel, R.M.A., Penninga, D., Rozeboom, H.J., Kalk, K.H., Dijkhuizen, L., and Dijkstra, B.W. (1996) Structure of cyclodextrin glucanotransferase complexed with maltononaose inhibitor at 2.6 Å resolution. Implication for product specificity. *Biochemistry* **35**, 4241–4249
26. Brunger, A.T., Kuriyan, J., and Karplus, M. (1987) Crystallographic *R* factor refinement by molecular dynamics. *Science* **235**, 458–460
27. Luzzati, V. (1952) Traitement statistique des erreurs dans la determination des structures cristallines. *Acta Cryst.* **5**, 802–810
28. Ramakrishnan, C. and Ramachandran, G.N. (1965) Stereochemical criteria or polypeptide and protein chain conformations. II. Allowed conformations for a pair of peptide units. *Biophys. J.* **5**, 909–933
29. Laskowski, R.A., MacArthur, M.W., Moss, D.S., and Thornton, J.M. (1993) PROCHECK: a program to check the stereochemical quality of protein structures. *J. Appl. Crystallog.* **26**, 283–291
30. Ishii, N., Haga, K., Yamane, K., Harata, K. (2000) Crystal structure of asparagine 233-replaced cyclodextrin glucanotransferase from alkalophilic *Bacillus* sp. #1011 determined at 1.9 Å resolution. *J. Mol. Recog.*, in press
31. Mosi, R., Sham, H., Uitdehaag, J.C.M., Ruiterkamp, R., Dijkstra, B.W., and Withers, S.G. (1998) Reassessment of acarbose as a transition state analogue inhibitor of cyclodextrin glycosyltransferase. *Biochemistry* **37**, 17192–17198